Nodal analysis of the human brain networks - a new way to couple function and structure

A Preprint

Viljami Sairanen [a,b]

[a]Baby Brain Activity Center, Children's Hospital,
Helsinki University Hospital and University of Helsinki, Finland

[b]Radiology, Hämeenlinna Central Hospital, Hämeenlinna, Finland

2025-10-15

Abstract

Combining the functional and structural connectomes of the human brain on macro-scale could provide information on various brain diseases and conditions. Unfortunately, accomplishing such combination is not trivial as the connectomes are usually derived from different imaging and measuring modalities that are based on different biophysical effects. The functional connectome is typically obtained using fMRI, EEG,or MEG whereas the structural connectome relies on diffusion-weighted MRI tractography. This work proposes a new way to perform this coupling using an analogy between brain connectomes and electric circuit. The idea is that functional correlations are treated as potentials and structural connections are treated as resistances of a circuit. In a sense, the proposal is a macro-scale version of the Hodkin-Huxley model. This work demonstrates how the proposed function-structure coupling can be applied as filtering for tractography by studying the Default Mode

Network of a subject from the Human Connectome Project. To provide a ground-truth example, a phantom simulation is used to detail how the method can solve functional connections in direct and indirect structural connection situations. The method is also applied to a cohort of 207 subjects from HCP to combine their functional and structural connectivity matrices to demonstrate how this approach could be used in group-level analyses. Finally, the proposed model is used to predict subject-wise functional connectomes from structural connectivity data. Predictions matched the measured functional connectomes from the same subjects with approximately Pearson's r of 0.73 which is on the level or even surpassing many of the state-of-the art graph neural network (GNN) approaches.

Keywords tractography · filtering · brain connectivity · structure · function · diffusion MRI · resting-state fMRI

1 Introduction

A recent review Greaves et al. (2025) highlighted a key challenge that persist in brain connectivity studies: how the functional connectome could be coupled with the structural connectome? This is difficult because on the macroscale, functional interactions between different brain regions might not be supported by any direct structural connections - so how to choose which structural pathways are used for any given functional signal? This study proposes an idea that can combine connectomes in any structural network having potential applications in brain connectivity studies as well as in dMRI tractography.

Various computational models have been proposed to link the human brain structure and function. (Breakspear et al., 2010) Some focus on the dynamical changes in the brain with biophysical models linking the structure to functional fluctuations and others with more statistical approaches that link these two on connectivity matrix basis. (Damoiseaux and Greicius, 2009; Deco, 2015; Greicius et al., 2009; Hermundstad

et al., 2013; Huang and Ding, 2016; Liu et al., 2022; Sporns, 2013; Suárez et al., 2020). Artificial intelligence has also been tested on this task with mainly graph neural network (GNN) approaches. (Chen et al., 2024; Hong et al., 2023; Neudorf et al., 2022; Yang et al., 2022; Zalesky et al., 2024) However, the literature seemed to have gap as it seems that previous attempts to use nodal analysis to study brain networks has not been done while it has been used to study many other networks such as electrical circuits with success. (Ho et al., 1975; Wedepohl and Jackson, 2002)

The functional connectome or functional networks can be derived from statistical patterns (Rubinov and Sporns, 2010) detected in the brain using functional magnetic resonance imaging (fMRI) time series, electroencephalography (EEG), or magnetoencephalography (MEG). (Sporns, 2013). Typically the derived functional connectome depicts only the correlations between activities in different brain regions which means that this information alone cannot be used to imply causal relationships (Smith et al., 2011). Despite this, functional connectome has provided insights into the behavior, aging, and how various diseases and conditions can affect the human brain.

The structural connectome of the living human brain is derived using diffusion-weighted magnetic resonance imaging (dMRI) and tractography (Basser et al., 1994; Behrens and Sporns, 2012; Johansen-Berg and Rushworth, 2009; Le Bihan et al., 2001). The derived connectome depicts pathways in which water molecules can travel in the brain and is often assumed to remain relatively stable during short time periods. These pathways are often referred to as tractography streamlines. While streamlines do not directly imply that there would be a white matter tract or fiber, many studies have demonstrated that streamlines can be used to infer orientations and trajectories of white matter bundles. (Sporns, 2013) However, tractography has a tendency to produce many false positive streamlines (Maier-Hein et al., 2016) due to e.g., noise, measurement methods, and processing (Sairanen and Andersson, 2023) which complicate deductions from the results. Even with these complications, the structural connectome has provided new insights into the organization of the human brain in various conditions.

The proposal in this study is to construct the function-structure coupling using an analogy with a well-known natural phenomenon: electrical currents in a circuit. Similar analogy has been drawn before in a much smaller scale in classical Hodkin-Huxley model (Hodgkin and Huxley, 1952). This study focuses on a global brain networks and tractography and drives the coupling analogy from the Modified Nodal Analysis (MNA) (Ho et al., 1975; Wedepohl and Jackson, 2002) of electrical circuits. As far as the author is aware, this is the first time that MNA has been applied to study the human brain. Considering the existing literature, the current work should not be considered as a biophysical model but more as a mathematical abstraction that allows the linking between two connectomes.

In the proposed analogy, the structural connectome is treated as resistance and the functional connectome is treated as electrical potential in an electrical circuit. Using this formulation, the variable of interest, current, explains how the functional information propagates through the structural network. While the actual method of functional signal traversing the brain is an electro-chemical process, at the macro-scale this analogy could provide a close-enough approximation of the process. The predictive capabilities of the proposed method seem to align or even surpass the state-of-the art GNNs (Chen et al., 2024; Hong et al., 2023; Neudorf et al., 2022; Yang et al., 2022) providing support for the proposal. Moreover, this study demonstrates how this analogy can be used to select which tractography streamlines would be necessary for functional information flow as well as how this idea can be used to form a completely new contrast for connectome analyses opening new ways to study the human brain. The developed algorithm to compute this 'information current' is provided as a Python code. [1]

2 Methods

This section is separated into five parts. The theoretical framework used in the proposed function-structure coupling 2.1, single subject example of tractogram filtering

[1] https://github.com/vilsaira/FSC

in Default Mode Network (Raichle et al., 2001) analysis 2.2, a ground-truth phantom simulation 2.3, group-level analysis of 207 subjects of the Human Connectome Project (Van Essen et al., 2012) 2.4, and the predictivity of the proposed model 2.5

2.1 Proposed function-structure coupling

This subsection demonstrates how the Modified Nodal (MNA) Analysis (Ho et al., 1975; Wedepohl and Jackson, 2002) can be applied to study the living brain. In MNA, unknown variables are nodal voltages $\mathbf{u}$ and currents flowing through the independent voltage sources $\mathbf{i_v}$. Known variables, independent voltage sources $\mathbf{V}$ and resistances are $\mathbf{R}$ are derived from the functional and structural connectivity.

A voltage source matrix $\mathbf{V}$ is defined as the functional connectivity matrix. Meaning voltage sources can be defined in as many ways as the functional connectivity e.g., resting-state networks or a task-specific activity in fMRI, EEG, or MEG. In this adaptation, the voltage sources are independent. In the future, this could be changed to study causality between functional correlations.

A resistance matrix $\mathbf{R}$ is defined as the structural connectivity matrix. Meaning the resistance matrix can be defined based various tractography algorithms and their outputs e.g., the streamline length, average fractional anisotropy, or even degree of myelination in some cases. The restriction is that both the functional and structural connectivity matrices should be generated using the same brain segmentations or atlas and therefore have the same number of parcellations from the same structural locations.

In general, MNA can be expressed in a matrix form as follows (Wedepohl and Jackson, 2002):

$$\begin{bmatrix} \mathbf{G} & \mathbf{B} \\ \mathbf{C} & \mathbf{D} \end{bmatrix} \begin{bmatrix} \mathbf{u} \\ \mathbf{i_v} \end{bmatrix} = \begin{bmatrix} \mathbf{i} \\ \mathbf{v} \end{bmatrix} \tag{1}$$

,

with the conductance matrix $\mathbf{G}$, an incidence matrices $\mathbf{B}$ and $\mathbf{C}$, an association matrix between voltage sources and dependent voltage sources $\mathbf{D}$, vectors of nodal voltages $\mathbf{u}$, currents through voltages sources $\mathbf{i_v}$, independent current sources $\mathbf{i}$, and independent voltage sources $\mathbf{v}$ i.e. the vectorized functional correlations.

With assumptions that *i*) there are no dependent voltage sources $\mathbf{D} = \mathbf{0}$ and $\mathbf{C} = \mathbf{B}^\top$ and *ii*) there are no current sources $\mathbf{i} = \mathbf{0}$, equation 1 can be simplified to

$$\begin{bmatrix} \mathbf{G} & \mathbf{B} \\ \mathbf{B}^\top & \mathbf{0} \end{bmatrix} \begin{bmatrix} \mathbf{u} \\ \mathbf{i_v} \end{bmatrix} = \begin{bmatrix} \mathbf{0} \\ \mathbf{v} \end{bmatrix} \tag{2}$$

.

Conductance is the reciprocal of the resistance, therefore $\mathbf{G}$ can be calculated from the resistance matrix $\mathbf{R}$ with the following logic. The diagonal elements G_{ii} are the sum of all conductances connected to node i. All other elements ij with $i \neq j$ are the opposite of the sum of all conductances connected between nodes i and j ensuring the conservation of charge i.e. that the sum of currents entering and leaving any node is zero.

The incidence matrix $\mathbf{B}$ contains the information of positive and negative terminals in the circuit and has dimensions of the number of nodes N in the connectivity matrices times the number of voltage sources M. The number of voltage sources is the number of non-zero elements in the voltage matrix. While it is an arbitrary choice of which direction is positive or negative in the $\mathbf{B}$ matrix, in all cases $B_{ij} = -B_{ji}$.

nodal voltages $\mathbf{u}$ solved from equation 2, can be used to calculate the currents I flowing through each edge of the network using Ohm's law $I = \frac{U}{R}$ where U contains nodal voltages, and R contains resistances. If resistances are defined as a structural connectome, this yields a new connectivity matrix that describes how the functional information flows through the structural network. Alternatively, resistances can be defined as tractography streamlines resulting in streamline-wise currents which could be used to filter unnecessary streamlines as well as to visualize the pathways in the brain that carry the functional information.

2.2 Default Mode Network example

One subject from the Human Connectome Project was used as a case example as it provided both the preprocessed resting-state fMRI with independent component analysis (ICA) results and diffusion-weighted MRI data.

A Default Mode Network atlas (Smith and Nichols, 2009) was used to identify which of the the ICA terms represented the DMN with the highest correlation. The resulting subject-wise DMN mask was then separated into six regions of interests that were used to form the functional and structural connectivity matrices. The regions were associated wtih anatomical locations of the medial prefrontal cortex (mPFC), posterior cingulate cortex (PCC), left and right inferior parietal lobules (IPL), and left and right temporal lobes (TL). The strength of the functional connectivity was defined as Pearson's correlation coefficient between the average intensities of these regions from the fMRI time series.

MRtrix (Tournier et al., 2019) was used to perform multi-shell multi-tissue anatomically constrained whole-brain tractography (Dhollander et al., 2016; Smith et al., 2012). A total of a million streamlines were calculated with maximum and minimum lengths of 250 mm and 5 mm. Normalized white matter FOD cutoff was 0.05. The structural connectivity matrix by using the the number of streamlines between the DMN nodes as edge weights. With the electrical circuit analogy, this can be seen as multiple identical parallel wires between two nodes making it easy path for the current. In the future, this is definitely something to investigate further, i.e. this weight could be replaced by streamline myelination or some combination of multiple metrics of interest.

The functional and structural connectomes were coupled using the proposed method described in section 2.1 and the ensuing nodal voltages were used to calculate the current matrix. For the streamline-wise analysis, a Steiner tree algorithm (Kou et al., 1981) was applied to select the edges with the highest currents. The corresponding nodal voltages were then used to calculate the streamline-wise current weights.

2.3 Ground-truth simulation

The FiberCup phantom (Fillard et al., 2011; Poupon et al., 2010, 2008) was used as a ground-truth structure for this simulation as it provided simple structure that allowed both direct and indirect functional correlation simulations. The phantom was separated into five functional subnetworks depicted in figure 4 A. The first four subnetworks were direct networks meaning that each of the functional network node was connected with a direct structural pathway. The fifth subnetwork was an indirect with one intermediate node. The fourth network was the secluded U-shape of the phantom working as a simple sanity check of the results as it should not have any effect on the other networks.

The strength of the functional correlation (potential) in all the subnetworks was set as one. The structural connectome was obtained using CSD tractography in MRtrix (Tournier et al., 2019) to produce a million streamlines. Analysis was separated into two parts. First, to evaluate the global tractogram filtering and second, to evaluate the correctness of all the subnetworks.

2.4 Group studies

To illustrate how the proposed method could be applied to obtain a complimentary connectome matrix on a group level, a group of unrelated healthy adults ($n = 207$, with 83 males, ages ranging from 22 to 36 years with mean $\pm$ std being 28.73 ± 3.73) from the HCP (Larivière et al., 2021, 2020; Van Essen et al., 2012) was used. The average structural and functional connectivity matrices of this sample were obtained using the ENIGMA Toolbox (Larivière et al., 2021). For the complete details on how these matrices were calculated, please see the "Connectivity data for macroscale connectome models" section by Larivière et al. (2021). For the demonstration purposes, the default parcellation scheme (Desikan-Killiany) was selected resulting in 68 times 68 connectivity matrices. Functional and structural connectivity matrices were used to calculate the current matrix.

2.5 Prediction functional correlations from structural connectome

This section investigates if the proposed model can be used to predict functional connections from the structural information. The study setup used the group-level functional and structural information from the group used in section 2.4 to obtain a template for the function-structural coupling model. Additional three subjects with structural and functional data from the HCP were used to evaluate the predictions.

The structural processing of the subjects was the same as used in the section 2.2 but instead of using the default mode network parcellations, the Desikan-Killiany cortical atlas was used as it would match the template's topology. The atlas parcellations were used to calculate the structural connectome based on the number of streamlines between each segment and the functional connectome based on the Pearson's correlation between the resting-state fluctuations in different segments. Correlation coefficients were transformed in to z-scores to match the data from the template.

The proposed method was used to predict subject-wise z-scores (functional correlations) from their respective structural connectomes using the template based function-structure coupling parameters. Since the three subjects also had resting-state fMRI data available, a direct comparison between the predicted and measured functional correlations was be done and evaluated using Pearson's correlation coefficient.

3 Results

A single subject (100307) and a dataset of an unrelated cohort of 207 healthy adult subjects from the Human Connectome Project (Larivière et al., 2021; Van Essen et al., 2012) were used in this study. The human examples provided real world demonstrations of the applicability of the proposed method and the predictive capability of the model. Complementary to human data, a simulation based on the FiberCup phantom (Fillard et al., 2011; Poupon et al., 2010, 2008) was used to provide a more intuitive demonstration of the method with known ground-truth specifications.

3.1 Default Mode Network example

An estimate for the location of the DMN nodes in the subject's brain was obtained by finding which ICA volume had the highest correlation with the DMN atlas (Smith and Nichols, 2009). This volume was spatially smoothed and thresholded to obtain subject-wise DMN nodes shown in figure 1. The six nodes found for this experiment roughly represent the medial prefrontal cortex (mPFC), posterior cingulate cortex (PCC), left and right inferior parietal lobules (IPL), and left and right temporal lobes (TL). This experiment is not aimed to describe how the DMN should be defined but to demonstrate how the proposed coupling algorithm could be applied to study any such network combination.

The subject's DMN mask was used to find all dMRI tractography streamlines that were connected to the DMN and are shown in figure 3 A. This tractogram was then filtered based on the function-structure coupling with streamlines that had zero or near zero current removed as shown in figure 2 B. Furthermore, the streamline-wise currents were used as the colormap in the latter image to visualize the parts of the structural network that carry most of the functional information. the functional information. Figure 3 demonstrates how the streamline-wise currents can be visualized together with the nodal potentials.

3.2 Ground-truth simulation

While the FiberCup phantom (Fillard et al., 2011; Poupon et al., 2010, 2008) can be seen as a simple toy example, it provides a known ground-truth structure that is simple enough to understand the results intuitively. The diffusion-weighted data of the phantom was appended with five functional subnetworks as shown in 4 A. The whole tractogram of the phantom is shown in figure 4 B with clearly all streamlines staying inside the phantom's 'white matter'.

Function-structure coupling was used to filter the whole tractogram in figure 4 C. As seen in the image, the unnecessary structural part of the phantom (in context of the simulated functional networks) is visibly missing from the results. This indicates that

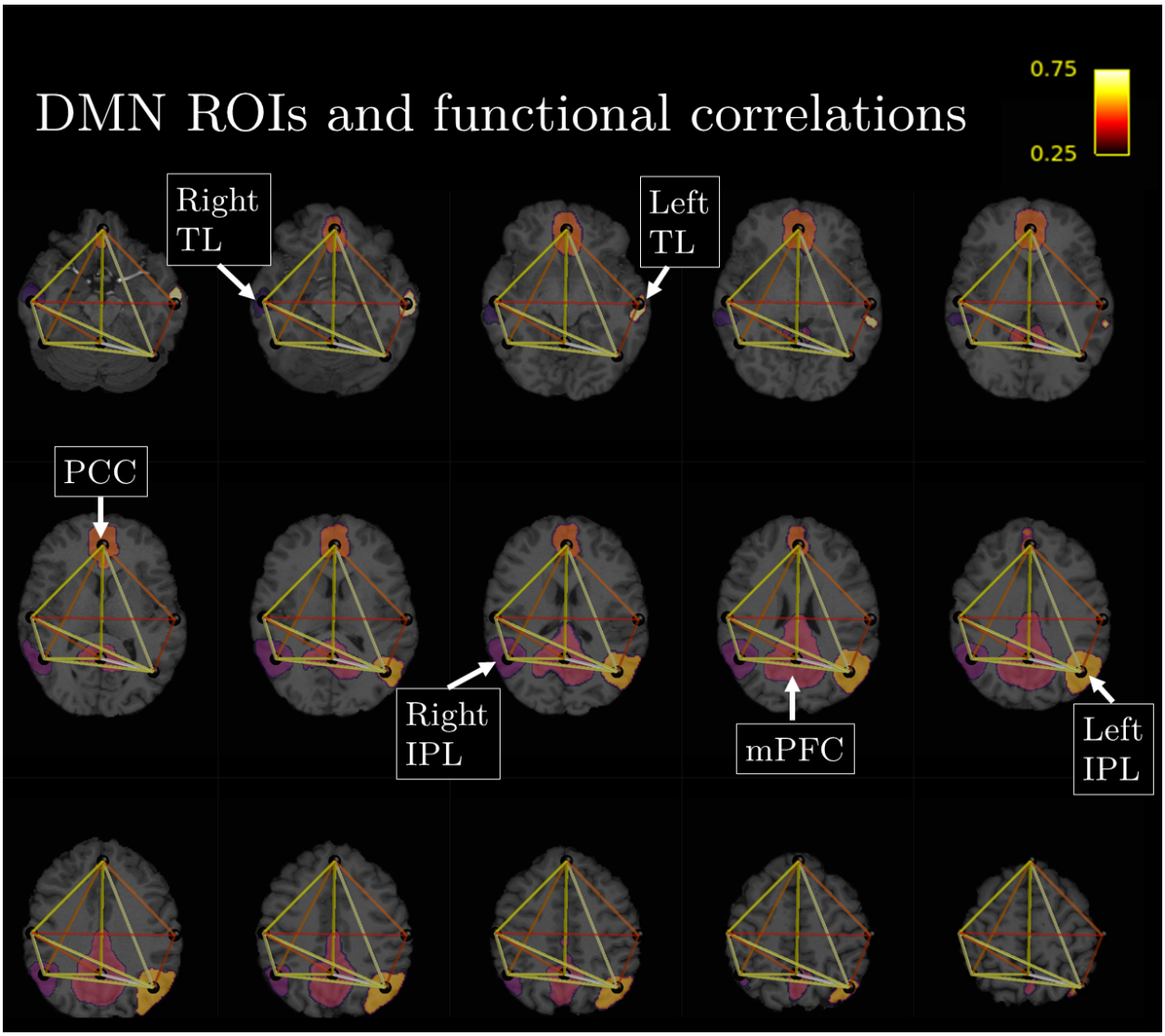

Figure 1: Visualization of the subject's Default Mode Network. The six regions of interest reflecting the network roughly are shown with different colours. The medial prefrontal cortex (mPFC), posterior cingulate cortex (PCC), left and right inferior parietal lobules (IPL), and left and right temporal lobes (TL). Respective functional network is depicted with a graph whose edge colour indicates functional correlations.

the algorithm can correctly detect which streamlines are necessary and optimal for the functional information flow.

A further analysis of the five functional subnetworks is shown in figure 5. All five subnetworks are identified correctly without any false-positive structural connections. Even the case of indirect connection via the opposite side of the phantom, the proposed algorithm correctly identifies the correct pathway.

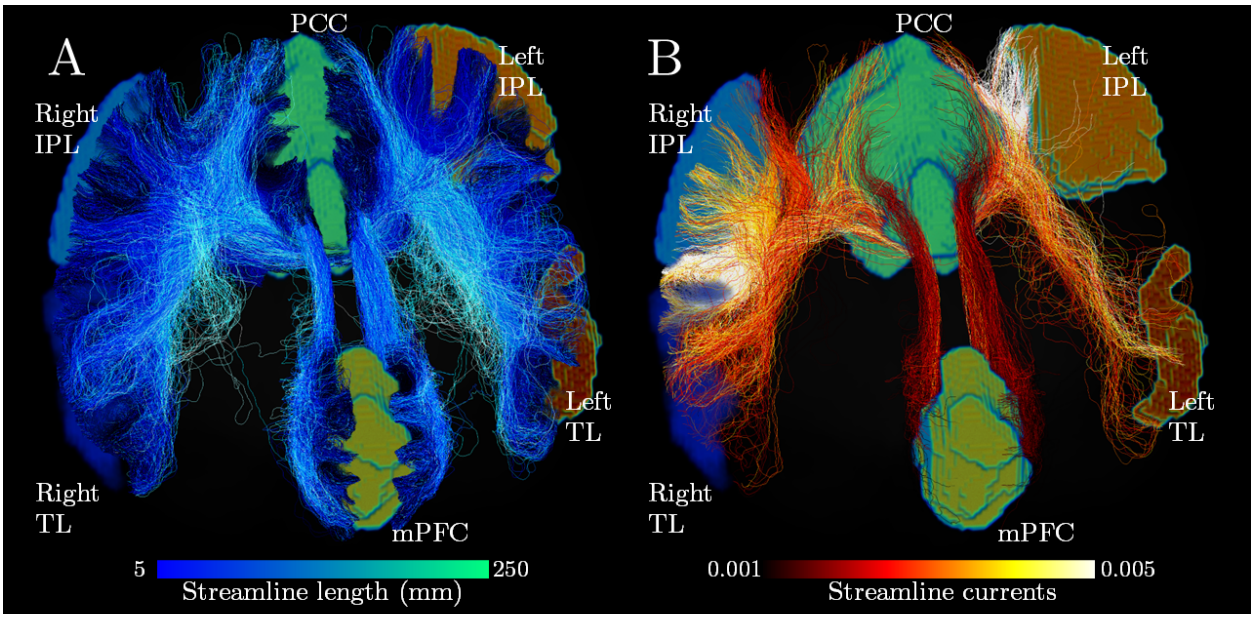

Figure 2: The proposed function-structure coupling can be used to filter tractograms. In this example, the default mode network defined by six brain regions PCC, mPFC, left and right IPL, and left and right TL is interconnected by the tractogram on the left (A). The blue-cyan colormap represents the length of the streamline in mm. By applying FSC (B), a notable amount of streamlines is pruned away as streamlines that do not carry meaningful current.

3.3 Group studies

Functional and structural connectivity matrices from 207 unrelated healthy adults from the Human Connectome Project (Van Essen et al., 2012) were used to calculate average functional and structural matrices using the ENIGMA Toolbox (Larivière et al., 2021). These average connectivity matrices were used to demonstrate the general feasibility of the proposed function-structure coupling.

In figure 6, the functional (red) and structural (blue) connectome are shown together with the resulting current (green) connectome. Notably, the novel connectome seem more sparse than either of other two. This could indicate, that many functional signals traverse via the same structural paths.

3.4 Prediction functional correlations from structural connectome

Figure 7 demonstrates the predictive capability of the proposed method. Three subjects from the HCP were used to calculate subject-wise functional connectomes and

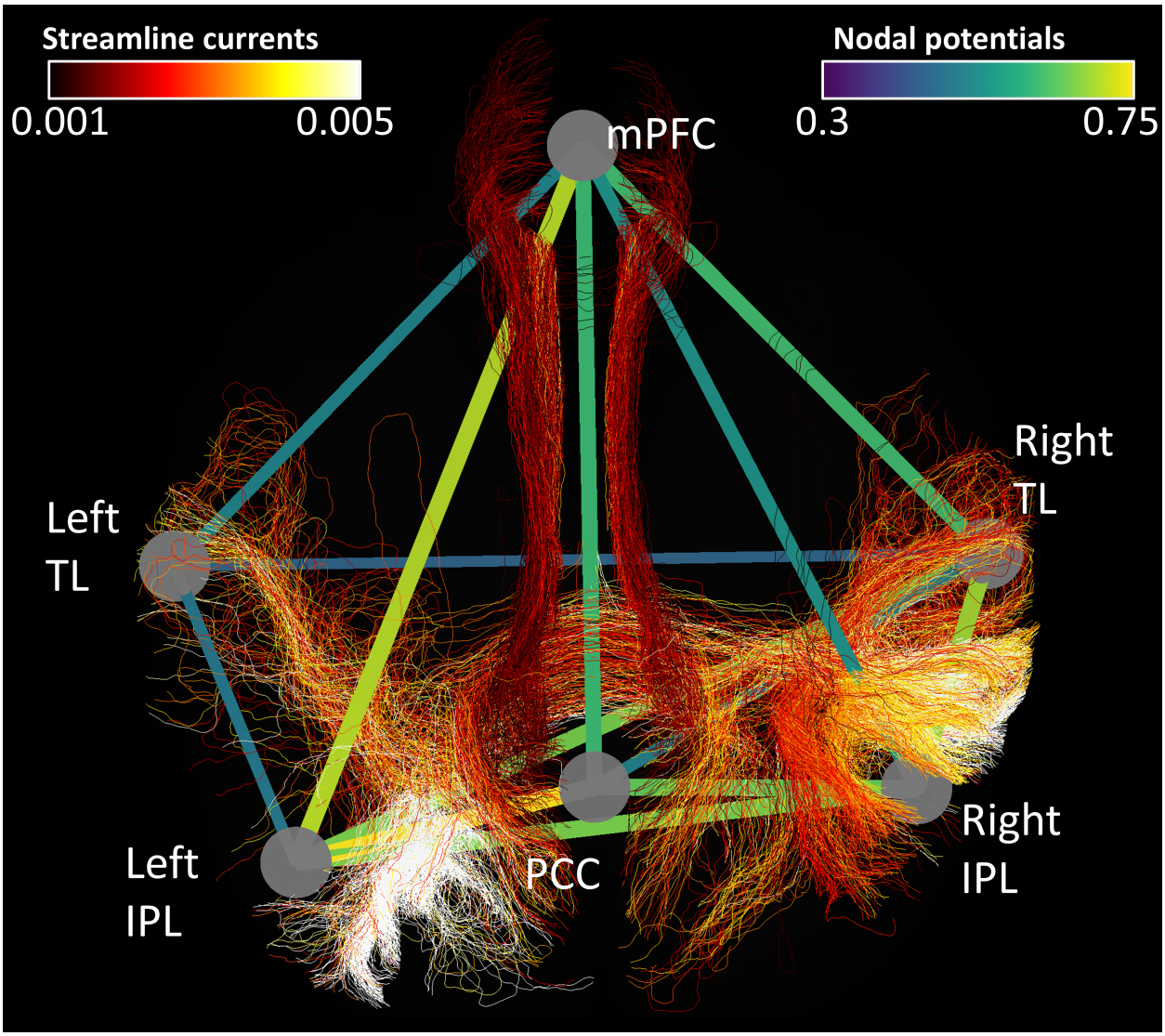

Figure 3: Obtained nodal voltages can be visualized together with the streamline-wise currents. In this example, subject's DMN is visualized by showing the nodal voltages as a graph with edges representing the voltage drop between each node. On top of this, a tractogram with streamlines colored by the streamline-wise currents. This type of visualization could be applied to any network and it is not limited to resting-state analyses.

compared to predictions made using the proposed method and subject-wise structural connectomes. The average correlation between predictions and measurements was 0.73 measured using Pearson's correlation coefficient.

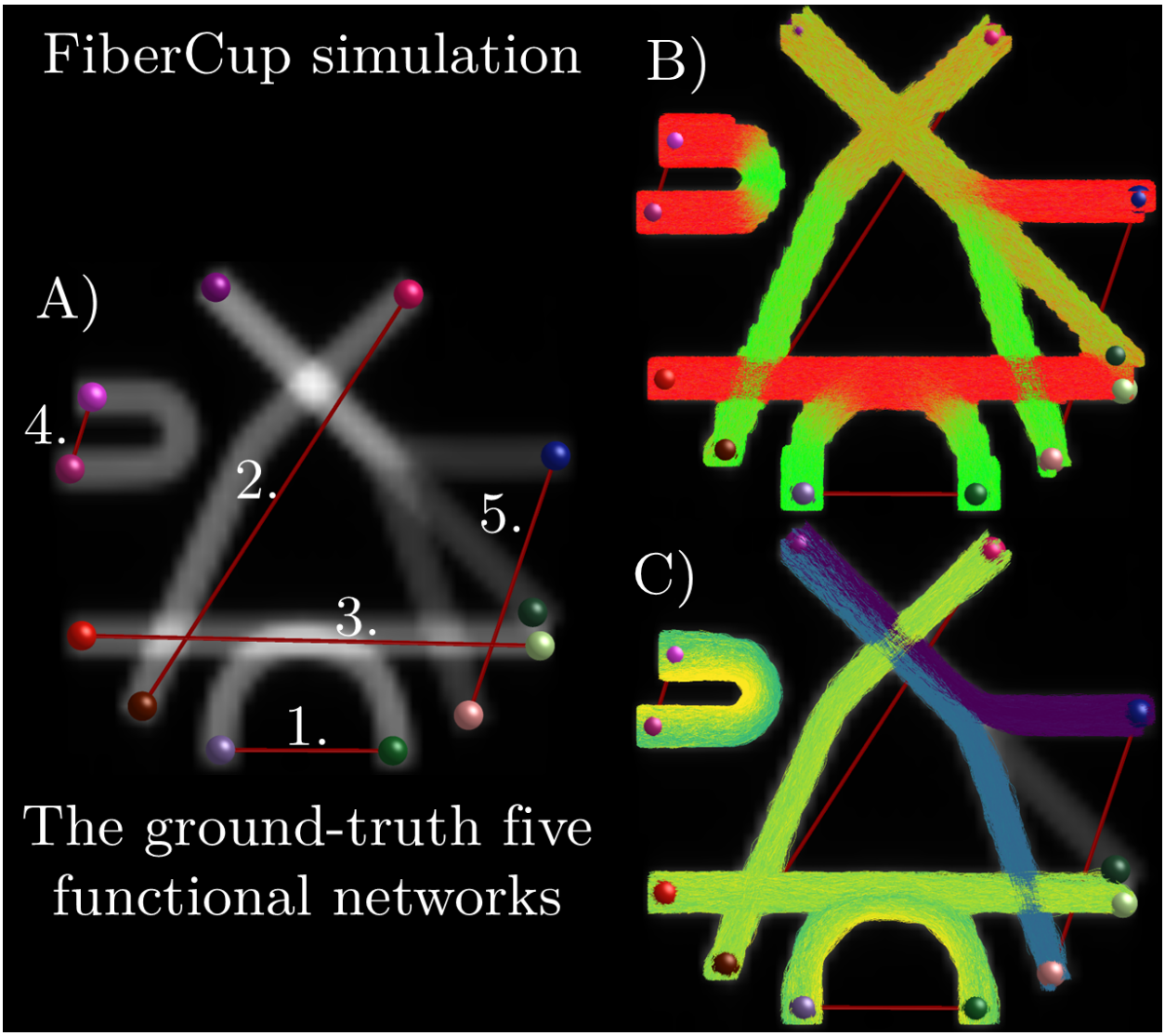

Figure 4: The ground-truth phantom simulation. A) The FiberCup phantom was separated into five simulated functional networks of which the fifth was an indirect connection i.e. there is no direct structural connection between the nodes. B) Whole tractogram of the phantom depicts the expected structure. C) The proposed method is used to filter the whole tractogram. The unnecessary structural part of the phantom is visibly missing from the results indicating that the algorithm can correctly detect which streamlines are necessary and optimal for the functional information flow.

4 Discussion

This study set out to investigate if an analysis method used to study electrical circuits (Modified Nodal Analysis, MNA) (Ho et al., 1975; Wedepohl and Jackson, 2002) could be used to study the macro-scale connectivity of the living human brain. With the predictive capabilities being on the same level with the state-of-the art graphical

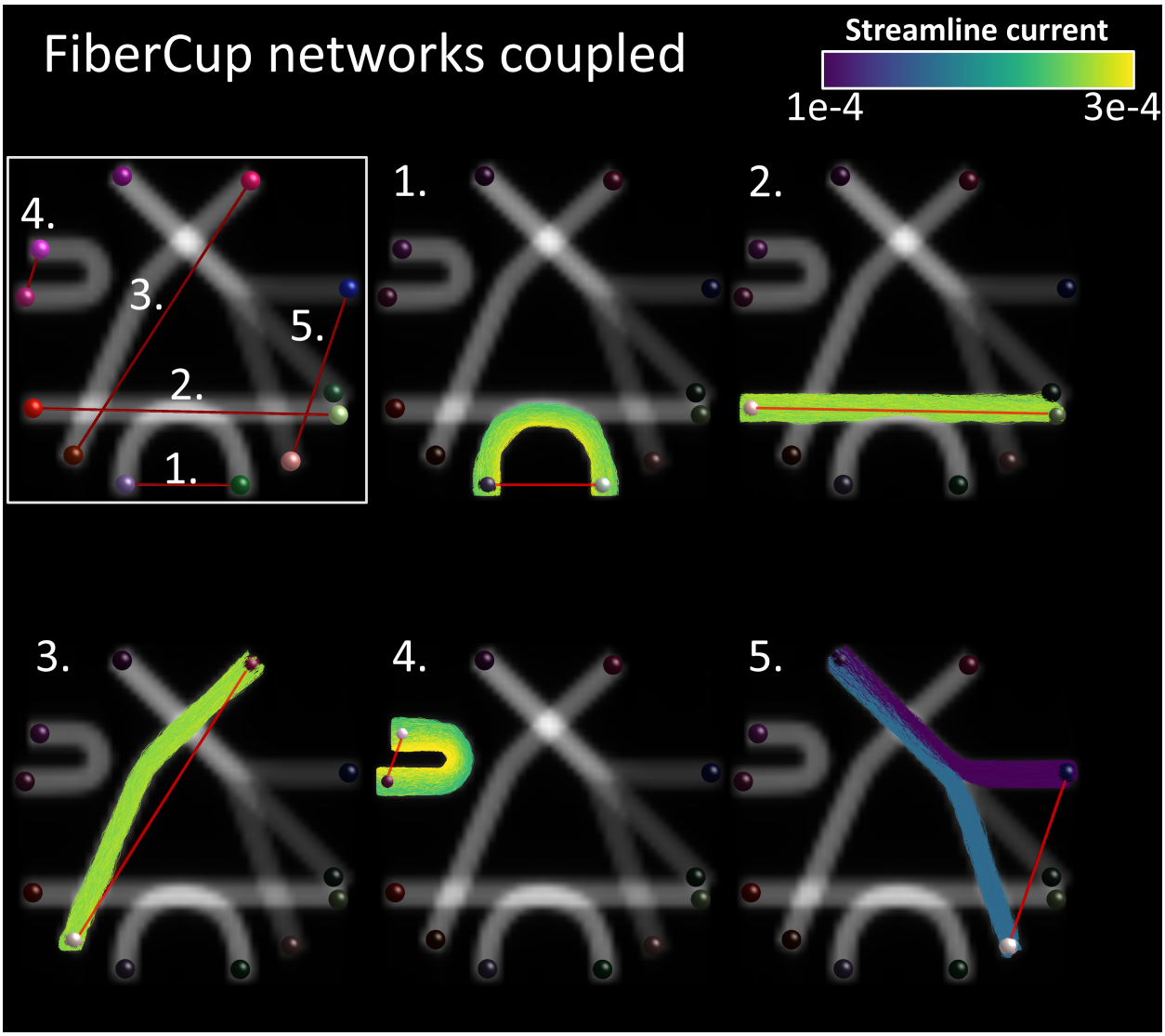

Figure 5: A further analysis of the five functional subnetworks in the ground-truth simulation. On the left top, the simulation setup is repeated. As seen in all subnetwork images, the proposed method correctly identifies the optimal pathway between any two nodes. Even the case with indirect connection via the opposite side of the phantom, the algorithm can find the connecting path. The color bar indicates the streamline-wise current which is notably smaller for the fifth subnetwork as the resistance in that network was higher due to longer travel path.

neural network (GNN) methods (Chen et al., 2024; Hong et al., 2023; Neudorf et al., 2022; Yang et al., 2022; Zalesky et al., 2024) and having additional applications in tractography, it is reasonable to conclude that modified nodal analysis could provide useful insights in analysis of brain networks. Considering the proposal is somewhat similar to the classical Hodkin-Huxley model (Hodgkin and Huxley, 1952), it is

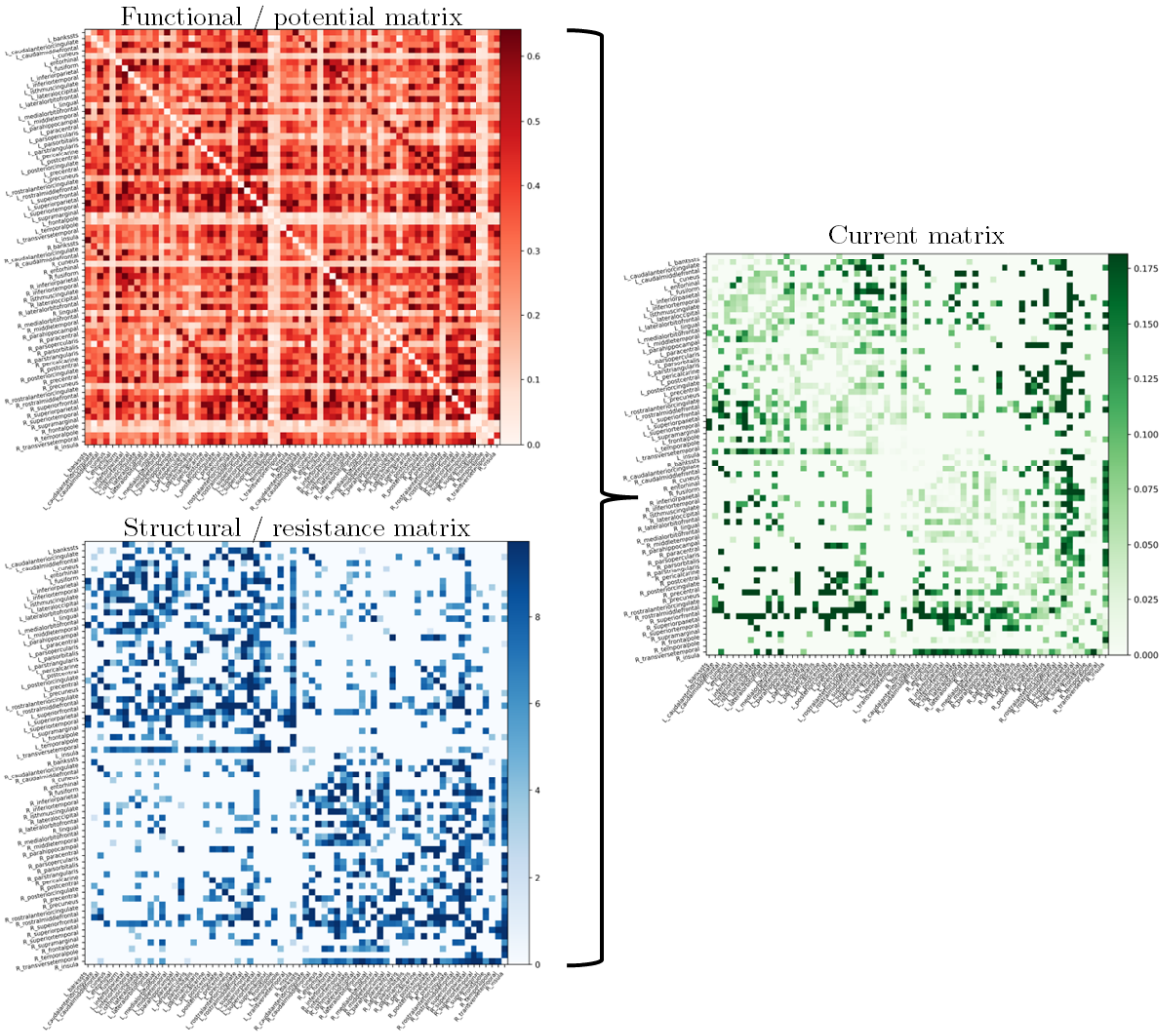

Figure 6: A new connectome 'contrast' can be produced by the proposed function-structure coupling method. Functional (red) and structural (blue) connectivity matrices can be used as a basis to calculate the corresponding current (green) connectome. This figure demonstrates that connectomes calculated from a large cohort can be studied with the proposed method.

reasonable to assume that this model too can be adjusted to obtain even better accuracy and therefore perhaps surpassing the GNN methods.

As shown in figure 7, the predictive capability of this method is already on similar level with the current state-of-the art deep learning methods with Pearson's correlation between prediction and measurement being 0.73 on average. A recent summary of AI based predictions (Zalesky et al., 2024) detailed prediction capabilities on individual

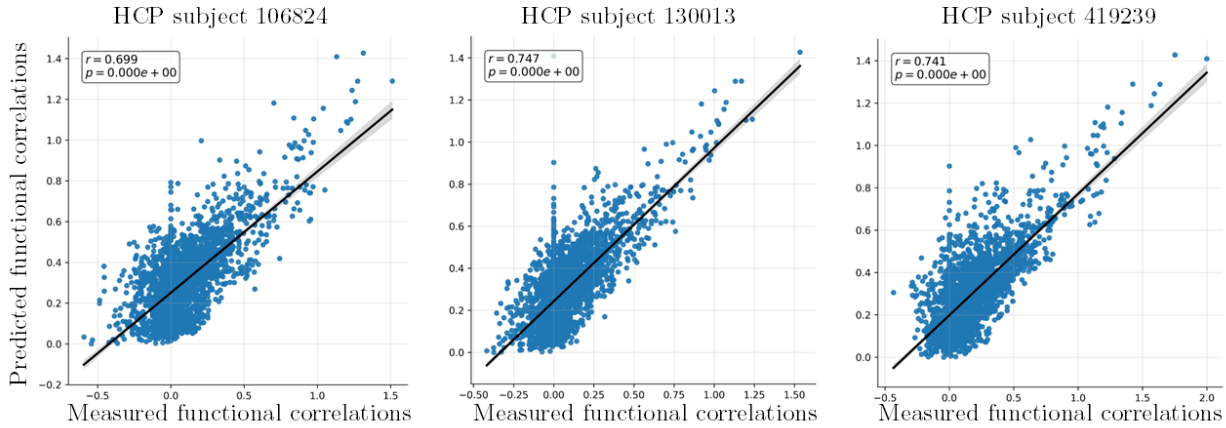

Figure 7: Results of subject-wise functional connectome predictions. Each plot shows the measured functional correlations (as z-scores) on the x-axis and the predicted functional correlations (as z-scores) on the y-axis. Pearson's correlation was used the evaluate the level of correlation.

level ranging from 0.5 to 0.8 measured using Pearson's correlation. For example, all graph neural network (GNN) based approaches (Chen et al., 2024; Hong et al., 2023; Neudorf et al., 2022; Yang et al., 2022) provided very similar (0.57 to 0.72) predictive capabilities on the individual level with the proposed approach.

Along with the predictive capabilities, the proposed function-structure coupling can be used to as additional information in tractogram filtering as shown in the phantom example 5. For example, compared to structural filtering algorithms on the same phantom (e.g. (Daducci et al., 2014)), the proposed method removed all false-positive findings. Not surprisingly, additional information used in filtering is beneficial. In the future, a more complex structural phantom simulations (e.g. (Schiavi et al., 2020)) along with biophysical dynamic functional modelling (Breakspear, 2017) could be performed to further benchmark the applicability of the proposed model in various filtering algorithms (Sairanen et al., 2021; Smith et al., 2015).

Streamwise information flow demonstrated in 3 could be beneficial for example in along-stream analyses (Colby et al., 2012) or tractometry (Chamberland et al., 2021). Being able to locate which white matter structures are used to propagate the functional information might reveal new insights in diseases that hamper that process. For

example, aphasia patients are a very diverse group with changes in different parts of the white matter (Sihvonen et al., 2024). By identifying what parts of the functional information flow are obstructed or start to improve due to rehabilitation, a more patient specific care could be planned.

The proposed function-structure coupling produces effectively an adjacency matrix, therefore existing network analysis tools, including GNNs, could be readily applied to study it further (Sporns, 2013). Similarly, existing tractography visualization tools can readily be applied to display the streamline-wise currents as shown in figure 3. The open source code provided as part of this study readily integrates with these tools that already exist in the computational neuroscience community.

If this model holds the scrutiny of the neuroscience community, theoretically it should be relatively simple to extend into dynamic models with time and event dependent voltage sources as well. This could provide a new opening for the dynamic brain modelling (Breakspear, 2017; Breakspear et al., 2010; Deco, 2015) and causality of functional effects (Friston, 2011) with the help of existing methods in dynamic circuit analyses. However, it should be kept in mind that the proposed method is limited by all the inaccuracies and assumptions that affect the functional and structural connectivity analyses.

In summary, this work combined functional and structural brain connectomes using an analogy with an electric circuit. This method provided a novel brain connectivity matrix that represents how the functional information flows in the structural brain network. The predictive capability of the proposed method was on the same level with the state-of-the art GNN approaches on the same topic. This study is limited by the availability of resources and should be seen as a proof-of-concept for a new method. Future studies with a more detailed simulations and patients affected by various diseases or conditions are needed to evaluate the method further. The conclusion of this study is that nodal analysis can be applied to study brain networks with possibility to obtain information not seen with other methods.

References

Basser, P., Mattiello, J., and LeBihan, D. (1994). MR diffusion tensor spectroscopy and imaging. *Biophysical Journal*, 66(1):259–267.

Behrens, T. E. J. and Sporns, O. (2012). Human Connectomics. *Current Opinion in Neurobiology*, 22(1):144–153.

Breakspear, M. (2017). Dynamic models of large-scale brain activity. *Nature neuroscience*, 20(3):340–352.

Breakspear, M., Jirsa, V., and Deco, G. (2010). Computational models of the brain: from structure to function.

Chamberland, M., Genc, S., Tax, C. M., Shastin, D., Koller, K., Raven, E. P., Cunningham, A., Doherty, J., van den Bree, M. B., Parker, G. D., et al. (2021). Detecting microstructural deviations in individuals with deep diffusion mri tractometry. *Nature computational science*, 1(9):598–606.

Chen, P., Yang, H., Zheng, X., Jia, H., Hao, J., Xu, X., Li, C., He, X., Chen, R., Okubo, T. S., et al. (2024). Group-common and individual-specific effects of structure–function coupling in human brain networks with graph neural networks. *Imaging Neuroscience*, 2:1–21.

Colby, J. B., Soderberg, L., Lebel, C., Dinov, I. D., Thompson, P. M., and Sowell, E. R. (2012). Along-tract statistics allow for enhanced tractography analysis. *Neuroimage*, 59(4):3227–3242.

Daducci, A., Dal Palù, A., Lemkaddem, A., and Thiran, J.-P. (2014). Commit: convex optimization modeling for microstructure informed tractography. *IEEE transactions on medical imaging*, 34(1):246–257.

Damoiseaux, J. S. and Greicius, M. D. (2009). Greater than the sum of its parts: a review of studies combining structural connectivity and resting-state functional connectivity. *Brain Structure and Function*, 213(6):525–533.

Deco, G. (2015). The dynamics of resting fluctuations in the brain. *BMC Neuroscience*, 16(Suppl 1):A2.

Dhollander, T., Raffelt, D., and Connelly, A. (2016). Unsupervised 3-tissue response function estimation from single-shell or multi-shell diffusion mr data without a co-registered t1 image. In *ISMRM workshop on breaking the barriers of diffusion MRI*, volume 5. Lisbon.

Fillard, P., Descoteaux, M., Goh, A., Gouttard, S., Jeurissen, B., Malcolm, J., Ramirez-Manzanares, A., Reisert, M., Sakaie, K., Tensaouti, F., et al. (2011). Quantitative evaluation of 10 tractography algorithms on a realistic diffusion mr phantom. *Neuroimage*, 56(1):220–234.

Friston, K. J. (2011). Functional and effective connectivity: a review. *Brain*, 1(1):13–36. MAG ID: 2061564920.

Greaves, M. D., Novelli, L., Mansour L., S., Zalesky, A., and Razi, A. (2025). Structurally informed models of directed brain connectivity. *Nature Reviews Neuroscience*, 26(1):23–41. Publisher: Nature Publishing Group.

Greicius, M. D., Supekar, K., Menon, V., and Dougherty, R. F. (2009). Resting-State Functional Connectivity Reflects Structural Connectivity in the Default Mode Network. *Cerebral Cortex*, 19(1):72–78. MAG ID: 2106396500.

Hermundstad, A. M., Bassett, D. S., Brown, K. K., Brown, K. S., Aminoff, E., Clewett, D., Freeman, S., Frithsen, A., Johnson, A., Tipper, C. M., Miller, M. B., Grafton, S. T., and Carlson, J. M. (2013). Structural foundations of resting-state and task-based functional connectivity in the human brain. *Proceedings of the National Academy of Sciences of the United States of America*, 110(15):6169–6174. MAG ID: 2002807356.

Ho, C.-W., Ruehli, A., and Brennan, P. (1975). The modified nodal approach to network analysis. *IEEE Transactions on Circuits and Systems*, 22(6):504–509. Conference Name: IEEE Transactions on Circuits and Systems.

Hodgkin, A. L. and Huxley, A. F. (1952). A quantitative description of membrane current and its application to conduction and excitation in nerve. *The Journal of Physiology*, 117(4):500–544.

Hong, Y., Cornea, E., Girault, J. B., Bagonis, M., Foster, M., Kim, S. H., Prieto, J. C., Chen, H., Gao, W., Styner, M. A., et al. (2023). Structural and functional connectome relationships in early childhood. *Developmental Cognitive Neuroscience*, 64:101314.

Huang, H. and Ding, M. (2016). Linking Functional Connectivity and Structural Connectivity Quantitatively: A Comparison of Methods. *Brain*, 6(2):99–108. MAG ID: 2229937548.

Johansen-Berg, H. and Rushworth, M. F. (2009). Using Diffusion Imaging to Study Human Connectional Anatomy. *Annual Review of Neuroscience*, 32(1):75–94. _eprint: https://doi.org/10.1146/annurev.neuro.051508.135735.

Kou, L., Markowsky, G., and Berman, L. (1981). A fast algorithm for steiner trees. *Acta informatica*, 15(2):141–145.

Larivière, S., Paquola, C., Park, B.-y., Royer, J., Wang, Y., Benkarim, O., Vos de Wael, R., Valk, S. L., Thomopoulos, S. I., Kirschner, M., Lewis, L. B., Evans, A. C., Sisodiya, S. M., McDonald, C. R., Thompson, P. M., and Bernhardt, B. C. (2021). The ENIGMA Toolbox: multiscale neural contextualization of multisite neuroimaging datasets. *Nature Methods*, 18(7):698–700. Number: 7 Publisher: Nature Publishing Group.

Larivière, S., Rodríguez-Cruces, R., Royer, J., Caligiuri, M. E., Gambardella, A., Concha, L., Keller, S. S., Cendes, F., Yasuda, C., Bonilha, L., Gleichgerrcht, E., Focke, N. K., Domin, M., von Podewills, F., Langner, S., Rummel, C., Wiest, R., Martin, P., Kotikalapudi, R., O'Brien, T. J., Sinclair, B., Vivash, L., Desmond, P. M., Alhusaini, S., Doherty, C. P., Cavalleri, G. L., Delanty, N., Kälviäinen, R., Jackson, G. D., Kowalczyk, M., Mascalchi, M., Semmelroch, M., Thomas, R. H., Soltanian-Zadeh, H., Davoodi-Bojd, E., Zhang, J., Lenge, M., Guerrini, R., Bartolini, E., Hamandi, K., Foley, S., Weber, B., Depondt, C., Absil, J., Carr, S. J. A., Abela, E., Richardson, M. P., Devinsky, O., Severino, M., Striano, P., Tortora, D., Hatton, S. N., Vos, S. B., Duncan, J. S., Whelan, C. D., Thompson, P. M., Sisodiya, S. M., Bernasconi, A., Labate, A., McDonald, C. R., Bernasconi, N., and Bernhardt, B. C.

(2020). Network-based atrophy modeling in the common epilepsies: A worldwide ENIGMA study. *Science Advances*, 6(47):eabc6457. Publisher: American Association for the Advancement of Science.

Le Bihan, D., Mangin, J.-F., Poupon, C., Clark, C. A., Pappata, S., Molko, N., and Chabriat, H. (2001). Diffusion tensor imaging: Concepts and applications. *Journal of Magnetic Resonance Imaging*, 13(4):534–546. _eprint: https://onlinelibrary.wiley.com/doi/pdf/10.1002/jmri.1076.

Liu, Z.-Q., Vazquez-Rodriguez, B., Spreng, R. N., Bernhardt, B. C., Betzel, R. F., and Misic, B. (2022). Time-resolved structure-function coupling in brain networks. *Communications biology*, 5(1):532.

Maier-Hein, K. H., Neher, P. F., Jean-Christophe Houde, Houde, J.-C., Côté, M.-A., Garyfallidis, E., Jidan Zhong, Zhong, J., Jidan Zhong, Chamberland, M., Fang-Cheng Yeh, Yeh, F.-C., Lin, Y.-C., Qing Ji, Ji, Q., Reddick, W. E., Glass, J. O., David Chen, David Qixiang Chen, David Qixiang Chen, Chen, D., Chen, D., Yuanjing Feng, Feng, Y., Chengfeng, G., Wu, Y., Ma, J., Renjie, H., Li, Q., Carl-Fredrik Westin, Westin, C.-F., Samuel Deslauriers-Gauthier, Deslauriers-Gauthier, S., Gonzalez, J. O. O., Paquette, M., St-Jean, S., Gabriel Girard, Girard, G., François Rheault, Rheault, F., Sidhu, J., Chantal M. W. Tax, Tax, C. M. W., Fenghua Guo, Guo, F., Mesri, H. Y., Szabolcs Dávid, David, S., Froeling, M., Heemskerk, A. M., Alexander Leemans, Leemans, A., Boré, A., Pinsard, B., Christophe Bedetti, Bedetti, C., Desrosiers, M., Brambati, S. M., Brambati, S. M., Doyon, J., Sarica, A., Vasta, R., Cerasa, A., Aldo Quattrone, Quattrone, A., Yeatman, J. D., Khan, A. R., Hodges, W., Wes Hodges, Wes Hodges, Alexander, S. P., Simon Alexander, Simon Alexander, Alexander, S., David Romascano, Romascano, D., Barakovic, M., Auria, A., Esteban, O., Lemkaddem, A., Thiran, J.-P., Jean-Philippe Thiran, Jean-Philippe Thiran, Jean-Philippe Thiran, Cetingul, H. E., Cetingul, H. E., Odry, B. L., Mailhe, B., Nadar, M. S., Mariappan S. Nadar, Nadar, M. S., Pizzagalli, F., Prasad, G., Villalon-Reina, J. E., Galvis, J., Thompson, P. M., De Santiago Requejo, F., Laguna, P. L., Lacerda, L., Rachel Barrett, Barrett, R., Flavio Dell'Acqua, Dell'Acqua, F., Catani, M., Petit, L., Caruyer, E., Daducci, A., Dyrby, T. B., Holland-Letz, T., Hilgetag,

C. C., Stieltjes, B., Bram Stieltjes, and Descoteaux, M. (2016). Tractography-based connectomes are dominated by false-positive connections. *bioRxiv*, page 084137. MAG ID: 2550828940.

Neudorf, J., Kress, S., and Borowsky, R. (2022). Structure can predict function in the human brain: a graph neural network deep learning model of functional connectivity and centrality based on structural connectivity. *Brain Structure and Function*, 227(1):331–343.

Poupon, C., Laribiere, L., Tournier, G., Bernard, J., Fournier, D., Fillard, P., Descoteaux, M., and Mangin, J.-F. (2010). A diffusion hardware phantom looking like a coronal brain slice. In *Proceedings of the international society for magnetic resonance in medicine*, volume 18, page 581.

Poupon, C., Rieul, B., Kezele, I., Perrin, M., Poupon, F., and Mangin, J.-F. (2008). New diffusion phantoms dedicated to the study and validation of high-angular-resolution diffusion imaging (hardi) models. *Magnetic Resonance in Medicine: An Official Journal of the International Society for Magnetic Resonance in Medicine*, 60(6):1276–1283.

Raichle, M. E., MacLeod, A. M., Snyder, A. Z., Powers, W. J., Gusnard, D. A., and Shulman, G. L. (2001). A default mode of brain function. *Proceedings of the national academy of sciences*, 98(2):676–682.

Rubinov, M. and Sporns, O. (2010). Complex network measures of brain connectivity: Uses and interpretations. *NeuroImage*, 52(3):1059–1069.

Sairanen, V. and Andersson, J. (2023). Outliers in diffusion-weighted MRI: Exploring detection models and mitigation strategies. *NeuroImage*, 283:120397.

Sairanen, V., Ocampo-Pineda, M., Granziera, C., Schiavi, S., and Daducci, A. (2021). Incorporating outlier information into diffusion MR tractogram filtering for robust structural brain connectivity and microstructural analyses. Technical report. Company: Cold Spring Harbor Laboratory Distributor: Cold Spring Harbor Laboratory Label: Cold Spring Harbor Laboratory Section: New Results Type: article.

Schiavi, S., Ocampo-Pineda, M., Barakovic, M., Petit, L., Descoteaux, M., Thiran, J.-P., and Daducci, A. (2020). A new method for accurate in vivo mapping of human brain connections using microstructural and anatomical information. *Science advances*, 6(31):eaba8245.

Sihvonen, A. J., Pitkäniemi, A., Siponkoski, S.-T., Kuusela, L., Martínez-Molina, N., Laitinen, S., Särkämö, E.-R., Pekkola, J., Melkas, S., Schlaug, G., et al. (2024). Structural neuroplasticity effects of singing in chronic aphasia. *Eneuro*, 11(5).

Smith, R. E., Tournier, J.-D., Calamante, F., and Connelly, A. (2012). Anatomically-constrained tractography: improved diffusion mri streamlines tractography through effective use of anatomical information. *Neuroimage*, 62(3):1924–1938.

Smith, R. E., Tournier, J.-D., Calamante, F., and Connelly, A. (2015). SIFT2: Enabling dense quantitative assessment of brain white matter connectivity using streamlines tractography. *NeuroImage*, 119:338–351. MAG ID: 795339718.

Smith, S. M., Miller, K. L., Salimi-Khorshidi, G., Webster, M., Beckmann, C. F., Nichols, T. E., Ramsey, J. D., and Woolrich, M. W. (2011). Network modelling methods for FMRI. *NeuroImage*, 54(2):875–891.

Smith, S. M. and Nichols, T. E. (2009). Threshold-free cluster enhancement: addressing problems of smoothing, threshold dependence and localisation in cluster inference. *Neuroimage*, 44(1):83–98.

Sporns, O. (2013). Structure and function of complex brain networks. *Dialogues in Clinical Neuroscience*, 15(3):247–262.

Suárez, L. E., Markello, R. D., Betzel, R. F., and Misic, B. (2020). Linking Structure and Function in Macroscale Brain Networks. *Trends in Cognitive Sciences*, 24(4):302–315.

Tournier, J.-D., Smith, R., Raffelt, D., Tabbara, R., Dhollander, T., Pietsch, M., Christiaens, D., Jeurissen, B., Yeh, C.-H., and Connelly, A. (2019). Mrtrix3: A fast, flexible and open software framework for medical image processing and visualisation. *Neuroimage*, 202:116137.

Van Essen, D. C., Ugurbil, K., Auerbach, E. J., Behrens, T. E., Bucholz, R. D., R. Bucholz, Chang, A., Chen, L., Maurizio Corbetta, Corbetta, M., Della Penna, S., Curtiss, S. W., Della Penna, S., Feinberg, D. A., Glasser, M. F., Heath, A. C., Harel, N., Heath, A. C., Larson-Prior, L. J., Marcus, D. S., Michalareas, G., Moeller, S., Oostenveld, R., Petersen, S., Petersen, S. E., Prior, F. W., Schlaggar, B. L., Smith, S. M., Snyder, A. Z., Xu, J., and Yacoub, E. (2012). The Human Connectome Project: A data acquisition perspective. *NeuroImage*, 62(4):2222–2231. MAG ID: 2020519533.

Wedepohl, L. M. and Jackson, L. (2002). Modified nodal analysis: an essential addition to electrical circuit theory and analysis. *Engineering Science & Education Journal*, 11(3):84–92. Publisher: IET Digital Library.

Yang, H., Winter, S., Zhang, Z., and Dunson, D. (2022). Interpretable ai for relating brain structural and functional connectomes. *arXiv preprint arXiv:2210.05672*.

Zalesky, A., Sarwar, T., Tian, Y., Liu, Y., Yeo, B. T., and Ramamohanarao, K. (2024). Predicting an individual's functional connectivity from their structural connectome: Evaluation of evidence, recommendations, and future prospects. *Network Neuroscience*, 8(4):1291–1309.

5 Acknowledgements

V.S. was supported by the Orion Research Foundation sr and Instrumentarium Science Foundation sr. The authors wish to thank the Finnish Computing Competence Infrastructure (FCCI) for supporting this project with computational and data storage resources. Open access funded by Helsinki University Library.